Sorption of tylosin and sulfamethazine on solid humic acid

Xuetao Guo[1], Bei Tu[1], Jianhua Ge[1], Chen Yang[2],*, Xiaomei Song[1], Zhi Dang[2]

1. *School of Earth and Environment, Anhui University of Science and Technology, Huainan 232001, China*
2. *College of Environment and Energy, South China University of Technology, Guangzhou 510006, China*

ARTICLE INFO

ABSTRACT

Tylosin (TYL) and sulfamethazine (SMT) are ionizable and polar antimicrobial compounds, which have seeped into the environment in substantial amounts via fertilizing land with manure or sewage. Sorption of TYL and SMT onto humic acid (HA) may affect their environmental fate. In this study, the sorption of TYL and SMT on HA at different conditions (pH, ionic strength) was investigated. All sorption isotherms fitted well to the Henry and Freundlich models and they were highly nonlinear with values of n between 0.5 and 0.8, which suggested that the HA had high heterogeneity. The sorption of TYL and SMT on HA decreased with increasing pH (2.0–7.5), implying that the primary sorption mechanism could be due to cation exchange interactions between TYL^+/SMT^+ species and the functional groups of HA. Increasing ionic strength resulted in a considerable reduction in the K_d values of TYL and SMT, hinting that interactions between H bonds and π–π EDA might be an important factor in the sorption of TYL and SMT on HA. Results of Fourier transform infrared (FT-IR) and ^{13}C-nuclear magnetic resonance (NMR) analysis further demonstrated that carboxyl groups and O-alkyl structures in the HA could interact with TYL and SMT via ionic interactions and H bonds, respectively. Overall, this work gives new insights into the mechanisms of sorption of TYL and SMT on HA and hence aids us in assessing the environmental risk of TYL and SMT under diverse conditions.

© 2015 The Research Center for Eco-Environmental Sciences, Chinese Academy of Sciences. Published by Elsevier B.V.

Introduction

In recent years, pharmaceutical antibiotics including tylosin (TYL) and sulfamethazine (SMT) have been produced in large quantities and extensively used in the farming industry as veterinary therapeutic agents and growth promoters, which will be inevitably released into the environment and then generate potential ecological risk (Zhou et al., 2014). Actually, releases of antibiotics into various media (*i.e.*, water, soil, and sediment) and the consequent risks to various ecological receptors have been reported (Leone et al. 2014; Mutavdžić Pavlović et al. 2014; Wu et al. 2014). Therefore, understanding the environmental behavior of antibiotics is important for evaluating environmental and health impact of antibiotics.

Numerous studies have been focused on the sorption behaviors of TYL and SMT in manure and soils (Aust et al. 2008; Guo et al. 2014; Jeong et al. 2012; Pei et al. 2014; Zhang et al. 2011b, 2013). It was found that TYL and SMT could interact with the surfaces and functional groups in manure and soils such as minerals and HAs (Kolz et al. 2005; Sassman et al. 2007; ter Laak et al. 2006). They revealed that the sorption of TYL and SMT on clays was primarily due to cation exchange effects, especially under acidic conditions (Zhang et al. 2013). Moreover, van der Waals forces could also play an important role on the distribution of TYL and SMT in the soil and water (Aust et al.

2008; Halling-Sorensen et al. 2005; Pei et al. 2014; Sassman et al. 2007; ter Laak et al. 2006; Zhang et al. 2011b). Guo et al. (2013, 2014) reported that TYL and SMT sorption on goethite was positively correlated to the formation of surface complexes, π–π EDA interactions and hydrophobic interactions, which might contribute partially to the overall sorption. In fact, TYL and SMT, like most antibiotics, are ionic compounds. TYL is a weak base with a pK_a of 7.1 (Zhang et al. 2013). In acidic conditions, ionic bonds could form between protonated TYL and anionic components in soil and manure matrices. SMT is an amphoteric compound with pK_a values at 2.28 and 7.42 (Guo et al. 2013). The net charges of SMT at different pH levels would be more complicated and thus lead to heterogeneous sorption activities between SMT and solid phases. When TYL and SMT are released into the environment, they might be adsorbed by soils and sediments, which would be a major process affecting the transport and fate of antibiotics in the environment.

HAs are natural polymers with a broad molecular-weight distribution and high chemical heterogeneity. They consist mainly of a skeleton of cross-linked aromatic blocks that are full of carboxylic and phenolic groups (Minella et al. 2013). Sorption of antibiotics onto HA is a major process determining the fate and bioavailability of antibiotics in soils and sediments. Once antibiotics are released into the environment, they would interact with HA. As a consequence of the interaction, the environmental behavior would be altered (Leone et al. 2014). The pH of the environment could also affect existing TYL and SMT forms. Thus, sorption mechanisms might be different at different pH levels (Zhao et al. 2014b). On the other hand, many kinds of ions coexist with TYL and SMT in the environment; however, interactions of these ions with HA have not been well elucidated. In order to assess the environmental risks of TYL and SMT, the sorption mechanisms of TYL and SMT on HA were investigated.

The objective of this study is to assess the sorption behavior and mechanism of TYL and SMT on HA and to understand the effect of HA on their environmental fate. The influences of solution chemical factors (i.e., pH and ionic strength) on the sorption of TYL and SMT on HA were also investigated.

1. Materials and methods

1.1. Materials and preparation

Tylosin tartrate (purity > 95%) and sulfamethazine (purity > 99%) were purchased from Sigma-Aldrich Corporation (St Louis, MO, USA). Acetonitrile and formic acid (HPLC grade, Merck Chemicals Co. AQ5) were used as received. Pure water was prepared by a Milli-Q® water purification system (Millipore Co., Guangzhou, China). All the other chemicals were analytical reagent grade and used without further purification.

Primary stock solutions of TYL and SMT at 1000 mg/L were prepared with pure water and stored at 4°C for a maximum of 1 month. The working solutions were prepared by diluting stock solution using 0.01 mol/L KNO₃ solution.

HA (solid granules with particle size 0.5–2 μm) used in this study was obtained from JuFeng Chemical Corporation, Shanghai, China. The elemental composition of HA is: 52.37% C, 3.57% H, 36.12% O, and 1.80% N.

1.2. Chemical analysis

The concentrations of TYL and SMT in aqueous solution were measured by reverse-phase high-performance liquid chromatography (AS-2455Plus, JASCO, Tokyo, Japan) with a C_{18} column (5 μm, 4.6 × 250 mm; Agilent) and diode array UV detector (Pgeneral, Beijing, China) (wavelength at 290 nm for TYL and 264 nm for SMT). The mobile phase by volume (at a flow rate of 0.5 mL/min) for TYL was a 35:65 mixture of acetonitrile and an aqueous solution containing 0.01 mol/L KH_2PO_4 (pH = 2.0) while for SMT it was a mixture of acetonitrile and formic acid solution (0.05%, V/V) at a volumetric ratio of 60:40 with a flow rate of 1 mL/min. The injection volume was 20 μL. External standards of TYL and SMT (0.1–100 mg/L) were employed to establish a linear calibration curve and the sample concentrations were calculated from its integrated peak areas. The solid phase concentrations were calculated based on the mass balance of the solute between the two phases.

1.3. Sorption and desorption procedure

The sorption experiments were conducted using a batch equilibrium technique at 25°C and pH 7.0. The initial TYL and SMT concentrations were set from 0.5 to 50 mg/L. The background solution contained 0.003 mol/L NaN_3 to minimize bioactivity and 0.01 mol/L KNO_3 to adjust ionic strength. A predetermined amount of HA was mixed with the initial aqueous solution in completely mixed batch reactor systems with Teflon gaskets and mixed on a shaker at 150 r/min to reach sorption equilibrium. The sorption equilibrium time for TYL and SMT was 24 hr. After the sorption experiments, the screw cap vials were centrifuged at 4000 r/min for 30 min, and 1 mL of supernatant was transferred into a pre-weighed 1.5 mL amber glass vial for chemical analyses. Each concentration level, including blanks, was run in triplicate. KOH or HNO_3 solutions were used for pH adjustment.

Desorption experiments were performed with a single cycle decant refill technique (Ramaswamy et al. 2012). In brief, after completion of the sorption test, each completely mixed batch reactor was weighed. Subsequently, the supernatant in each reactor was emptied with a pipette and then the reactor with the precipitates was weighed so that the amount of TYL/SMT-free background aqueous solution could be calculated and added. Afterwards, the reactor was reweighed, capped, and placed in the shaker for desorption experiments. After mixing under the same conditions, the tubes were centrifuged and set upright for 12. The supernatant was withdrawn from each reactor for quantification of TYL/SMT in the solution phase.

1.4. Sorption isotherm models

The equilibrium sorption data was fitted using Henry (Eq. (1)) and Freundlich (Eq. (2)) models (Ji et al. 2009):

$$q_e = k_d C_e \tag{1}$$

$$q_e = k_f C_e^n \tag{2}$$

where C_e (mg/L) and q_e (mg/kg) are the equilibrium concentration of TYL/SMT in the liquid phase and solid phase, respectively; k_d (L/kg) is the distribution coefficient of solute between

soil and water. k_f (mg/kg)/(mg/L)^n is the capacity affinity parameter and n (dimensionless) is the exponential parameter. Parameters were estimated by nonlinear regression weighted by the dependent variable.

1.5. Spectrum analysis

HA, TYL/SMT and TYL/SMT sorbed onto HA were measured using a Fourier Transform Infrared (FT-IR) spectrometer (Thermo, Nicolet 380, USA). The samples were dried under vacuum until constant weight was achieved and then mixed with KBr powder (1%) prior to the FT-IR spectra analysis.

1.6. ^{13}C NMR analysis

Solid-state ^{13}C NMR spectra were obtained at the ^{13}C resonance frequency of 400 MHz on an ACANCE III spectrometer (Bruker BioSpin, Switzerland), equipped with a double resonance HX probe. The samples were confined in a zirconium oxide rotor with an external diameter of 2.5 mm. The cross-polarization magic angle spinning CPMAS technique was applied with a contact time of 1 msec, a spinning speed of 15 kHz MAS and a pulse delay of 2.

2. Results and discussion

2.1. Sorption and desorption isotherms of TYL and SMT on HA

Sorption and desorption isotherms of TYL and SMT on HA are presented in Fig. 1. The fitting parameters are summarized in Table 1. It was observed that the two models were suitable to describe sorption and desorption behavior of TYL and SMT on HA, as indicated by the high regression coefficient ($R^2 > 0.98$).

The estimated k_d were 386.1 L/kg and 216.4 L/kg for TYL and SMT sorption on HA respectively, which was higher than those reported for sorption of TYL and other sulfonamides in soils (Białk-Bielińska et al. 2012; Thiele-Bruhn et al. 2004; Tolls 2001; Zhang et al. 2011b). Zhang et al. (2011b) reported that the k_d for TYL on agricultural soils ranged from 1.7 to 12 L/kg. Lertpaitoonpan et al. (2009) reported k_d values for SMT ranging

from 0.23 to 3.91 L/kg in different soils. In our previous studies, the estimated k_d for TYL and SMT on goethite were 11.54 and 5.08 L/kg (Guo et al. 2013). These results suggest that not only the physico-chemical properties of TYL and SMT but also the properties of HA play a crucial role in the fate of TYL and SMT in soil ecosystems. The mobility of TYL and SMT might be small for soils rich in HA.

The nonlinearity coefficient n values for TYL and SMT on HA were less than 1, indicating nonlinear sorption of TYL and SMT on HA. Although nonlinearity was also observed in the sorption isotherms of tetracyclines and norfloxacin onto HA (Zhang et al. 2012), the n values for those previous studies were much closer to 1 than these of TYL and SMT in this study. The lower n value indicated more heterogeneous glassy, hard or condensed sorption domains in the sorbents and higher sorption site energy distribution (Zhang et al. 2011a). As the n values are generally related to the site energy distribution, the smaller n values denoted more heterogeneous sorption sites. The heterogeneous nature of HA made it more difficult to adsorb additional molecules at a high TYL and SMT concentration. This might occur when specific binding sites become saturated and the remaining sites are much weaker in adsorbing the molecules (Zhang et al. 2011a). The k_f obtained in this study were 1610 and 839 (μg/g)/(mg/L)^n for TYL and SMT respectively, which were consistent with Gu et al. (2007).

Sorption and desorption isotherms are shown in Fig. 1. A significant sorption and desorption hysteresis was also

Table 1 – List of tylosin (TYL) and sulfamethazine (SMT) sorption and desorption isotherm parameters.

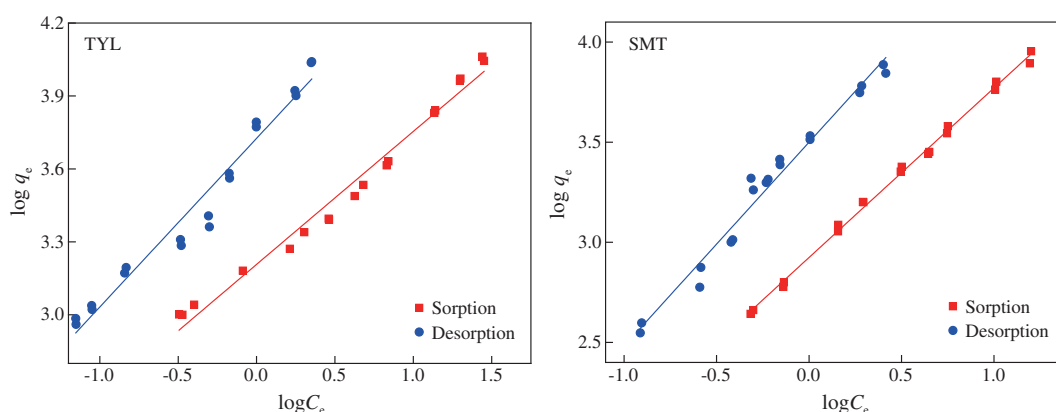|		Henry model		Freundlich model		
		k_d (L/kg)	R^2	n	k_f ((μg/g)/ (mg/L)^n)	R^2
TYL	Sorption	386.1	0.989	0.546	1610	0.980
	Desorption	4526	0.985	0.693	5308	0.964
SMT	Sorption	216.4	0.987	0.846	839	0.996
	Desorption	2881	0.981	1.018	3162	0.980

Fig. 1 – Sorption and desorption isotherms of tylosin (TYL) and sulfamethazine (SMT) on humic acid (HA). Contact time for TYL and SMT were 24 hr; equilibrium pH for TYL was 2.5 and for SMT was 3.0; temperature = 25°C; ionic strength 0.01 mol/L KNO₃.

observed. The sorption–desorption apparent hysteresis index (H) was expressed by Eq. (3) (Gu et al. 1995):

$$H = n_d/n \qquad (3)$$

where n and n_d are the Freundlich parameters for sorption and desorption, respectively.

The calculated H were 1.27 and 1.20 for TYL and SMT, which were greater than 1, indicating that sorption–desorption hysteresis occurred. This was consistent with a previous report (Wu et al. 2013), which reported the sorption–desorption hysteresis of ciprofloxacin on clay mineral. Apparent hysteretic behaviors might be attributed to a significant fraction of TYL and SMT that was irreversibly retained on HA by chemical entrapment or conformational changes after HA interacted with TYL.

2.2. Effect of pH on TYL and SMT sorption on HA

The sorption isotherms of TYL and SMT at different pH values are shown in Fig. 2. The sorption of TYL and SMT onto HA appeared to be strongly pH-dependent. The sorption decreased as pH increased for both TYL and SMT, which was consistent with previous observations for cyromazine and norfloxacin sorption to HAs (Zhang et al. 2012; Zhao et al. 2014a).

The Henry model and Freundlich model were employed to fit data at different pH values. It was observed that the two models were suitable to describe sorption well, with correlation coefficients R^2 consistently >0.980 (Table 2). It was evident that the sorption parameters of k_d and k_f for TYL and SMT decreased with increasing pH from 2.5 to 7.5. Trends in sorption correlated well with the variation of TYL and SMT speciation with pH and the availability of cation exchange sites in the HA. This further indicated that sorption was driven primarily via cation exchange at low pH values. Generally, cation interactions with HA occurred at optimal pH values when both the cationized sorbate species and the cationized HA carboxyl groups reached the maximum amounts (Zhao et al. 2014a). In this study, TYL and SMT sorption were maximized under acidic conditions when a large fraction of TYL and SMT existed as cations. On the other hand, the pK_a value for the carboxyl group of HA was 3.6, indicating that the cationized carboxyl group of HA reached a maximum at pH below 3.6 (Carmosini and Lee 2009). The low sorption at the pH

Table 2 – Effect of pH the sorption isotherm parameters of TYL and SMT.

	pH	Henry model		Freundlich model		
		k_d (L/kg)	R^2	n	k_f ((μg/g)/(mg/L)^n)	R^2
TYL	3	386.1	0.989	0.546	1610	0.980
	4	352.7	0.987	0.438	1432	0.983
	5	297.5	0.988	0.372	1187	0.987
	7	268.4	0.991	0.324	986	0.985
SMT	2.5	235.6	0.986	0.889	1013	0.991
	3.5	216.4	0.987	0.846	839	0.996
	5.5	189.7	0.992	0.765	764	0.986
	7.5	165.4	0.983	0.683	687	0.983

values when neutral forms of TYL and SMT were the important species demonstrated that the neutral species were not favorable for HA sorption. This confirmed that the sorption was dominated by cation exchange on positively charged sites on HA. It can also be inferred that cation exchange interactions might involve the amidogen of TYL and SMT and the positively charged carboxylic groups in HA, especially in the pH range of 2.0–3.5. A similar result was also observed in the sorption of fluoroquinolones on humic materials (Zhang et al. 2012).

The fraction of protonated carboxylic groups on the surface of HA increased as pH declined, which indicated that intra and intermolecular H-bonding can facilitate the formation of a more condensed conformation for HA and provide more sorption sites for TYL and SMT. As the solution pH increased, the concentration of TYL$^+$ decreased and the neutral species of TYL became dominant. As a result, the electrostatic interactions between TYL$^+$ and HA weakened. Sorption of neutral TYL on HA might be dominated by hydrophobic interactions, which controlled the overall sorption of non-ionic and less polar organic chemicals on soils and sediments. Similarly for SMT, when the pH value was in the range of 3.0–8.0, the neutral form would be dominant, and hydrophobic interactions may be the dominant sorption mechanisms (Guo et al. 2014).

2.3. Effect of ionic strength on TYL and SMT sorption on HA

Fig. 3 shows that the sorption isotherms of TYL and SMT on HA at different KNO$_3$ concentrations with a constant pH-value
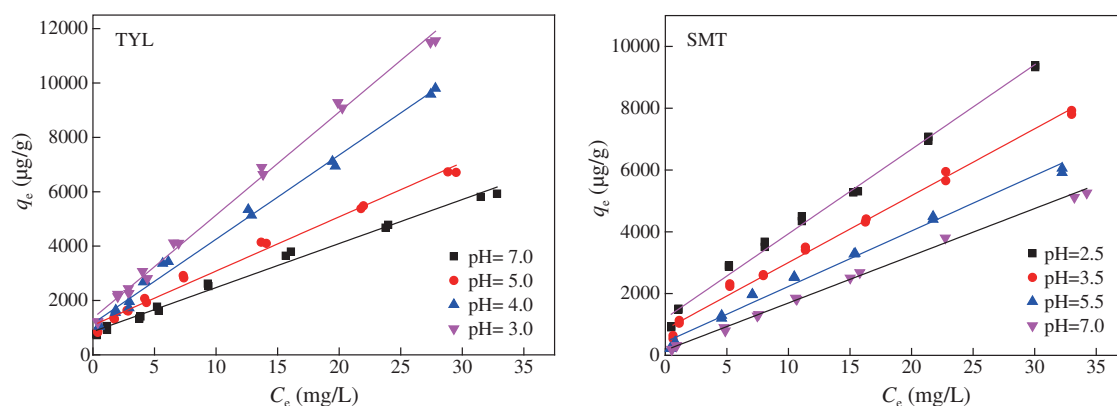

Fig. 2 – Sorption of TYL and SMT on HA at different pH values. Contact time for TYL and SMT were 24 h; temperature = 25°C; ionic strength 0.01 mol/L KNO$_3$.
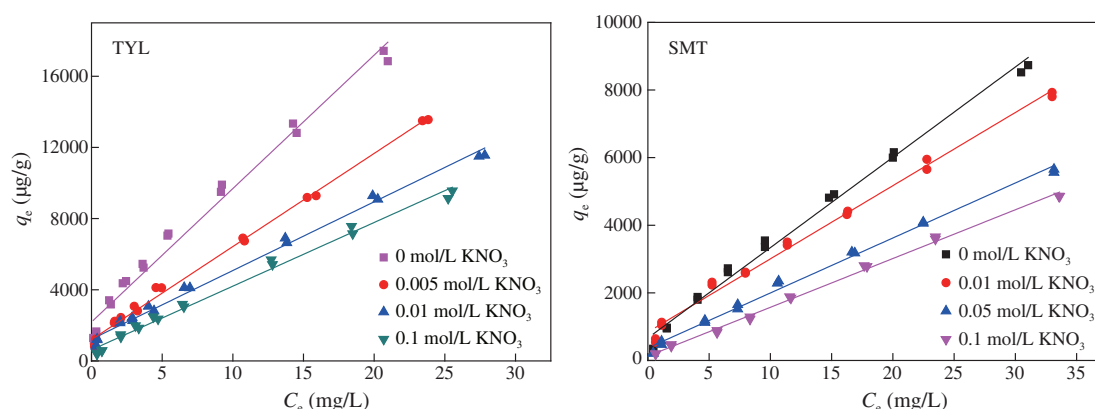
Fig. 3 – Sorption of TYL and SMT on HA at different ionic strength levels. Contact time for TYL and SMT were 24 hr; equilibrium pH for TYL was 2.5 and for SMT was 3.0; temperature = 25°C.

of 3.0. The sorption of TYL and SMT decreased significantly with reduced k_d and k_f values as K^+ concentration increased. These results indicated that the a higher K^+ concentration led to lower sorption of TYL and SMT on HA, which also agreed with the result that cation exchange was the dominant process in the sorption (Zhao et al. 2014a). The decreased n values (Table 3) with increasing K^+ concentration further demonstrated the competitive effect of K^+ during the sorption process.

The sorption capacity of HA was largely dependent on the ionization and surface charge. Most protons on the carboxyl groups of HA were dissociated at pH 5.0, forming negatively charged HA surfaces. When the K^+ concentration was increased, a large quantity of K^+ would be adsorbed to form outer-sphere complexes in the β layer, resulting in a decrease of negative charges and a compression of the double layer. In other words, the decrease in TYL and SMT sorption with increasing K^+ concentration might be due to K^+ occupying sorption sites on HA that should have been available for TYL and SMT. Hence, if cation exchange was the controlling process, decreasing the competing inorganic cation concentration should increase the sorption at a given pH. Otherwise, the complexation with K^+ might alternatively enhance sorption by

forming a bridge on the surface, which has been observed for sorption of tetracycline antibiotics onto pure clays and humic material (Ahmed et al. 2015; Zhang et al. 2013).

2.4. FT-IR analysis

The interactions between TYL/SMT and HA were investigated by comparing the spectra of adsorbed TYL/SMT on HA to those of free TYL/SMT and HA under the same analysis conditions. The FT-IR spectra of free TYL and SMT, free HA, and TYL/SMT- HA complexes at pH 3.0 are shown in Fig. 4.

Compared with the spectrum of free HA, the spectra for HA-adsorbed TYL at pH 3.0 had no new peaks, indicating that there were no structure changes accompanying sorption of TYL on HA. However, a strong absorption peak at 1716 cm^{-1} corresponded to the C=O stretch of the –COH group for free TYL. The peak position at 1701 cm^{-1} was increased, indicating that the –COH groups of TYL and the –COOH groups HA were probably involved in the sorption interaction via H-bonding (Zhang et al. 2012; Zhao et al. 2014a). For SMT, however, the spectra for HA-adsorbed SMT at pH 3.0 had many new peaks that were similar to the spectrum of free SMT, indicating that SMT had been integrated into the structure of HA. A broad band at 3208 cm^{-1} primarily corresponding to O–H stretching and secondarily to N–H stretching indicated the activated bands of SMT combined with HA (Li et al. 2013). A similar peak position for the –COOH group in the spectrum of SMT on HA at pH 3.0 shifted slightly from 1686 cm^{-1} to 1658 cm^{-1}, indicating that the -COOH groups of HA were probably involved in the sorption interaction via H-bonding (Guo et al. 2014). Based on the reported pK_a value of carboxylic acid groups for HA (3.75) in this study, the formation of intermolecular H-bonding between SMT and HA was feasible during the adsorption of SMT on HA at pH 3.0. Generally, deprotonation of the carboxylic group resulted in the C–O bond behaving more or less like a C=O bond with increasing pH in the solution, and thereby the absorbance in the C–O stretching region diminished. For the HA after sorption of SMT, two peaks at 1405 and 1304 cm^{-1} were assigned to asymmetric and symmetric stretching vibrations of the keto group involved in sorption. The peaks at 821, 702 and 621 cm^{-1}

| Table 3 – Effect of ionic strength the sorption isotherm parameters of TYL and SMT.						
	Ionic strength (mol/L)	Henry model		Freundlich model		
		k_d (L/kg)	R^2	n	k_f ((μg/g)/ (mg/L)^n)	R^2
TYL	0	457.6	0.994	0.673	1923	0.986
	0.005	423.7	0.987	0.602	1752	0.992
	0.01	386.1	0.989	0.546	1610	0.980
	0.1	375.4	0.982	0.487	1487	0.987
SMT	0	258.4	0.991	0.889	986	0.986
	0.01	216.4	0.987	0.846	839	0.996
	0.05	176.5	0.986	0.754	765	0.982
	0.1	154.2	0.981	0.672	681	0.989
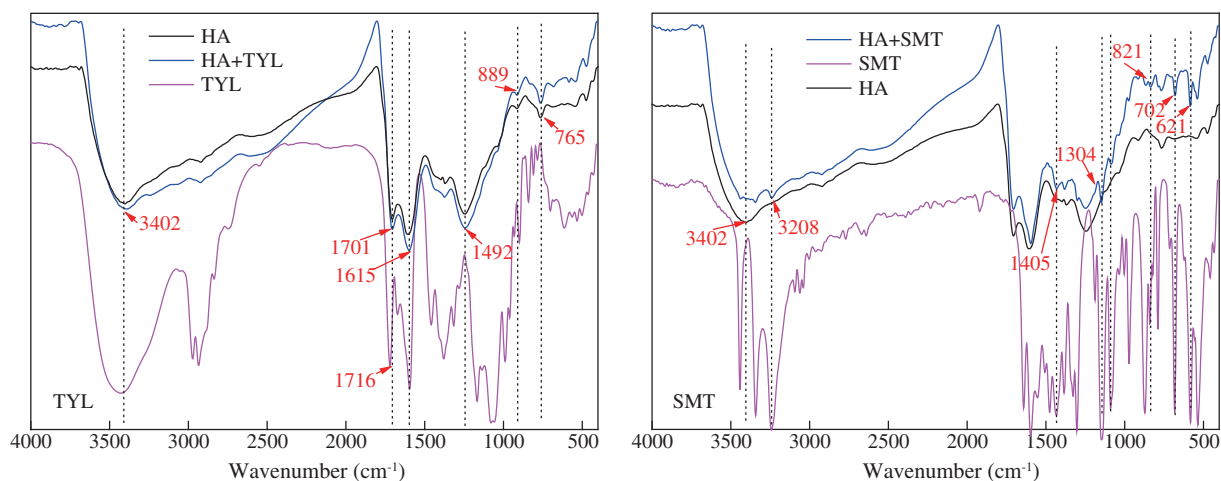
Fig. 4 – Fourier transform infrared spectra for free TYL and SMT, TYL/SMT–HA complex and free HA.

in the spectrum of HA after SMT sorption were assigned to the protonation of N in the benzene group, which indicated that the sorption mechanism of SMT on HA could also be explained by π–π EDA interaction, one of the driving forces for the sorption of organic chemicals with benzene rings on HA (Zhang et al. 2012; Zhao et al. 2014a). The benzene rings with N substituents in SMT could function as π electron acceptors due to the strong electron-withdrawing ability of N. The –OH groups on the HA surface could make the benzene rings of HA act as electron donors. Thus, significantly enhanced SMT sorption on HA by formation of a π–π bond was expected. However, the π–π bond was significantly depressed between SMT and HA because the –COOH groups made HA benzene rings act as electron acceptors. Hydrogen bonds play important roles in the process of polar organic pollutant sorption on carbon nanomaterials (Lin et al. 2012). Functional groups of organic chemicals could act as hydrogen bonding donors and form hydrogen bonds with the HA, where the benzene rings could act as hydrogen-bonding acceptors.

2.5. ^{13}C-NMR analysis

To explore possible contributions of specific parts of HA to the sorption of TYL/SMT, the ^{13}C NMR spectra of TYL/SMT–HA complexes and free HA at pH 3.0 were measured and shown in Fig.5. Within the chemical shift range of 0–250 ppm, the NMR spectra are divided into seven regions according to the chemical shift as follows: C atoms at 0–45 ppm are assigned to alkyl C, 45–60 ppm methoxyl/N-alkyl C, 60–110 ppm O-alkyl C, 110–140 ppm aromatic C–H, 140–160 ppm phenolic C, 160–185 ppm carboxylic C, and 185–220 ppm carbonyl C (Jacobs et al. 2010). The structural carbon distribution (%) of TYL/SMT–HA complex and free HA at pH 5.0 was calculated from solid-state CP-MAS ^{13}C NMR, and the results are shown in Table 4.

The content of polar C (phenolic C + carboxylic C + carbonyl C) was 13.81% for free HA. The distribution of N-alkyl C of the HA decreased greatly from 3.27% to 0.38% and 0.34% after sorption of TYL and SMT respectively, which suggested that the N-alkyl of HA played an important role in the sorption. This result was consistent with the FTIR results, which showed that there were multiple active sorption sites for HA. Because of the cation exchange interactions of TYL and SMT with HA, the chemical shift of N-alkyl C changed to a smaller ppm. On the other hand, the aromatic C, phenolic C and carboxylic C showed apparent changes after sorption of TYL and SMT. These results indicated that the sorption interactions might have occurred on carbonyl groups via H-bonding and aromatic structures via the hydrophobic effect (Villaescusa et al. 2011). The carbonyl group of HA had been reported in previous studies to be the most important group for the sorption of ionic compounds, based on the different chemical shift regions distinguished by ^{13}C NMR (Xu et al. 2005).
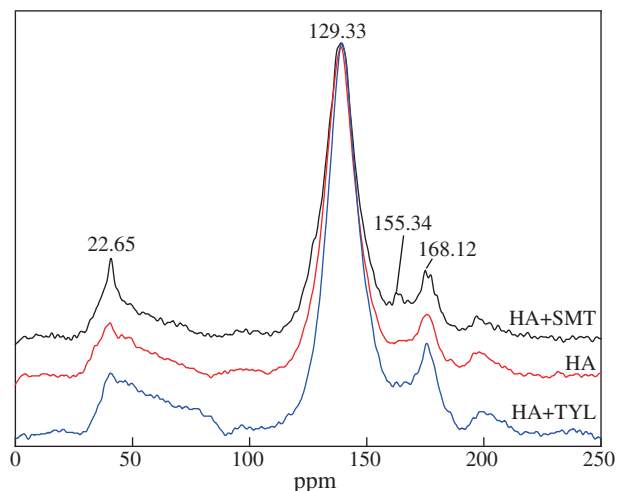

Fig. 5 – Solid-state ^{13}C NMR spectra of free HA and TYL/SMT–HA complex.

Table 4 – Structure carbon distribution (%) of free HA and TYL/SMT–HA complex at pH 5.0.						
Sample	Carbonyl C 185–220 ppm	Carboxylic C 160–185 ppm	Phenolic C 140–160 ppm	Aromatic C 110–140 ppm	O-alkyl C 60–110 ppm	N-alkyl C 45–60 ppm	Alkyl C 0–45 ppm
HA	1.24	7.23	4.34	82.34	0.58	3.27	4.13
HA-SMT	1.12	8.35	6.58	75.12	0.81	0.38	7.24
HA-TYL	0.98	8.11	5.92	79.57	0.63	0.34	5.15

3. Conclusions

HA was considered as a special type of sorbent because of its strong sorption affinity and capacity for organic contaminants. The present study showed that HA has a high sorption capacity TYL and SMT with highly nonlinear sorption, which was probably due to its heterogeneous surface. The Henry and Freundlich models fitted well with all sorption isotherms under different pH values and ionic strengths. The pH and ionic strength obviously had a noticeable effect the sorption of TYL and SMT on HA, which indicated that the primary sorption mechanism was cation exchange and π-π EDA interaction for TYL and SMT. FTIR and ^{13}C-NMR analysis showed that the amino groups of TYL and SMT were the active sorption sites for interaction with HA, while the carboxyl group and the O-alkyl structure of HA interacted with TYL and SMT via ionic interaction and H bonds. Overall, the results in the present study demonstrated the importance of HA as a sorbent phase for TYL and SMT and the strong influence of solution chemistry in TYL/SMT-HA sorption. These findings also provided a rational basis for evaluating conditions favorable for strong sorption of antibiotic pollutants onto humic materials.

Acknowledgments

R E F E R E N C E S

Ahmed, A.A., Thiele-Bruhn, S., Aziz, S.G., Hilal, R.H., Elroby, S.A., Al-Youbi, A.O., Leinweber, P., Kuehn, O., 2015. Interaction of polar and nonpolar organic pollutants with soil organic matter: Sorption experiments and molecular dynamics simulation. Sci. Total Environ. 508, 276–287.

Aust, M-O., Godlinski, F., Travis, G.R., Hao, X., McAllister, T.A., Leinweber, P., Thiele-Bruhn, S., 2008. Distribution of sulfamethazine, chlortetracycline and tylosin in manure and soil of Canadian feedlots after subtherapeutic use in cattle. Environ. Pollut. 156:1243–1251.

Białk-Bielińska, A., Maszkowska, J., Mrozik, W., Bielawska, A., Kołodziejska, M., Palavinskas, R., Stepnowski, P., Kumirska, J., 2012. Sulfadimethoxine and sulfaguanidine: their sorption potential on natural soils. Chemosphere 86, 1059–1065.

Carmosini, N., Lee, L.S., 2009. Ciprofloxacin sorption by dissolved organic carbon from reference and bio-waste materials. Chemosphere 77, 813–820.

Gu, B., Schmitt, J., Chen, Z., Liang, L., McCarthy, J.F., 1995. Adsorption and desorption of different organic matter fractions on iron oxide. Geochim. Cosmochim. Acta 59, 219–229.

Gu, C., Karthikeyan, K.G., Sibley, S.D., Pedersen, J.A., 2007. Complexation of the antibiotic tetracycline with humic acid. Chemosphere 66, 1494–1501.

Guo, X., Yang, C., Dang, Z., Zhang, Q., Li, Y., Meng, Q., 2013. Sorption thermodynamics and kinetics properties of tylosin and sulfamethazine on goethite. Chem. Eng. J. 223, 59–67.

Guo, X., Yang, C., Wu, Y., Dang, Z., 2014. The influences of pH and ionic strength on the sorption of tylosin on goethite. Environ. Sci. Pollut. Res. 21, 2572–2580.

Halling-Sorensen, B., Jacobsen, A.M., Jensen, J., Sengelov, G., Vaclavik, E., Ingerslev, F., 2005. Dissipation and effects of chlortetracycline and tylosin in two agricultural soils: a field-scale study in southern Denmark. Environ. Toxicol. Chem. 24, 802–810.

Jacobs, A., Helfrich, M., Hanisch, S., Quendt, U., Rauber, R., Ludwig, B., 2010. Effect of conventional and minimum tillage on physical and biochemical stabilization of soil organic matter. Biol. Fert. Soils. 46, 671–680.

Jeong, C.Y., Wang, J.J., Dodla, S.K., Eberhardt, T.L., Groom, L., 2012. Effect of biochar amendment on tylosin adsorption–desorption and transport in two different soils. J. Environ. Qual. 41, 1185–1192.

Ji, L., Chen, W., Duan, L., Zhu, D., 2009. Mechanisms for strong adsorption of tetracycline to carbon nanotubes: a comparative study using activated carbon and graphite as adsorbents. Environ. Sci. Technol. 43, 2322–2327.

Kolz, A.C., Ong, S.K., Moorman, T.B., 2005. Sorption of tylosin onto swine manure. Chemosphere 60, 284–289.

Leone, V., Iovino, P., Salvestrini, S., Capasso, S., 2014. Sorption of non-ionic organic pollutants onto a humic acids-zeolitic tuff adduct: thermodynamic aspects. Chemosphere 95, 75–80.

Lertpaitoonpan, W., Ong, S.K., Moorman, T.B., 2009. Effect of organic carbon and pH on soil sorption of sulfamethazine. Chemosphere 76, 558–564.

Li, J., Fu, J., Xiang, X., Wu, M., Liu, X., 2013. Kinetics, equilibrium, and mechanisms of sorption and desorption of 17 alpha-ethinyl estradiol in two natural soils and their organic fractions. Sci. Total Environ. 452, 404–410.

Lin, D., Tian, X., Li, T., Zhang, Z., He, X., Xing, B., 2012. Surface-bound humic acid increased Pb2+ sorption on carbon nanotubes. Environ. Pollut. 167, 138–147.

Minella, M., Merlo, M.P., Maurino, V., Minero, C., Vione, D., 2013. Transformation of 2,4,6-trimethylphenol and furfuryl alcohol, photosensitised by Aldrich humic acids subject to different filtration procedures. Chemosphere 90, 306–311.

Mutavdžić Pavlović, D., Ćurković, L., Blažek, D., Župan, J., 2014. The sorption of sulfamethazine on soil samples: isotherms and error analysis. Sci. Total Environ. 497–498, 543–552.

Pei, Z., Yang, S., Li, L., Li, C., Zhang, S., Shan, X.Q., Wen, B., Guo, B., 2014. Effects of copper and aluminum on the adsorption of sulfathiazole and tylosin on peat and soil. Environ. Pollut. 184, 579–585.

Ramaswamy, J., Prasher, S.O., Patel, R.M., 2012. Sorption and desorption of salinomycin sodium in clay, loamy sand, and sandy soils. Environ. Monit. Assess. 184, 5363–5369.

Sassman, S.A., Sarmah, A.K., Lee, L.S., 2007. Sorption of tylosin A, D, and A-aldol and degradation of tylosin A in soils. Environ. Toxicol. Chem. 26, 1629–1635.

ter Laak, T.L., Gebbink, W.A., Tolls, J., 2006. The effect of pH and ionic strength on the sorption of sulfachloropyridazine, tylosin, and oxytetracycline to soil. Environ. Toxicol. Chem. 25, 904–911.

Thiele-Bruhn, S., Seibicke, T., Schulten, H.R., Leinweber, P., 2004. Sorption of sulfonamide pharmaceutical antibiotics on whole soils and particle-size fractions. J. Environ. Qual. 33, 1331–1342.

Tolls, J., 2001. Sorption of veterinary pharmaceuticals in soils: a review. Environ. Sci. Technol. 35, 3397–3406.

Villaescusa, I., Fiol, N., Poch, J., Bianchi, A., Bazzicalupi, C., 2011. Mechanism of paracetamol removal by vegetable wastes: the contribution of pi–pi interactions, hydrogen bonding and hydrophobic effect. Desalination 270, 135–142.

Wu, Q., Li, Z., Hong, H., Li, R., Jiang, W.-T., 2013. Desorption of ciprofloxacin from clay mineral surfaces. Water Res. 47, 259–268.

Wu, D., Li, H., Liao, S., Sun, X., Peng, H., Zhang, D., Pan, B., 2014. Co-sorption of ofloxacin and Cu(II) in soils before and after organic matter removal. Sci. Total Environ. 481, 209–216.

Xu, D., Xu, Z., Zhu, S., Cao, Y., Wang, Y., Du, X., Gu, Q., Li, F., 2005. Adsorption behavior of herbicide butachlor on typical soils in China and humic acids from the soil samples. J. Colloid Interf. Sci. 285, 27–32.

Zhang, G., Zhang, Q., Sun, K., Liu, X., Zheng, W., Zhao, Y., 2011a. Sorption of simazine to corn straw biochars prepared at different pyrolytic temperatures. Environ. Pollut. 159, 2594–2601.

Zhang, Q., Yang, C., Dang, Z., Huang, W., 2011b. Sorption of tylosin on agricultural soils. Soil Sci. 176, 407–412.

Zhang, Q., Zhao, L., Dong, Y.H., Huang, G.Y., 2012. Sorption of norfloxacin onto humic acid extracted from weathered coal. J. Environ. Manag. 102, 165–172.

Zhang, Q., Yang, C., Huang, W., Dang, Z., Shu, X., 2013. Sorption of tylosin on clay minerals. Chemosphere 93, 2180–2186.

Zhao, L., Lin, Z.R., Dong, Y.H., 2014a. Sorption of cyromazine on humic acid: effects of pH, ionic strength and foreign ions. Environ. Sci. Pollut. Res. 21, 2688–2696.

Zhao, Y., Tong, F., Gu, X., Gu, C., Wang, X., Zhang, Y., 2014b. Insights into tetracycline adsorption onto goethite: experiments and modeling. Sci. Total Environ. 470, 19–25.

Zhou, D., Chen, B., Wu, M., Liang, N., Zhang, D., Li, H., Pan, B., 2014. Ofloxacin sorption in soils after long-term tillage: the contribution of organic and mineral compositions. Sci. Total Environ. 497, 665–670.